Schweizerische Eidgenossenschaft
Confédération suisse
Confederazione Svizzera
Confederaziun svizra

Eidgenössisches Departement für
Umwelt, Verkehr, Energie und Kommunikation UVEK

Bundesamt für Energie BFE

INTERMEDIATE TEMPERATURE FUEL CELLS BASED ON PROTON CONDUCTING ELECTROLYTES

Final Report

Prepared by

Sophie Duval
Peter Holtappels
Empa, Laboratory for High Performance Ceramics, Überlandstr. 129, CH-8600 Dübendorf

peter.holtappels@empa.ch

www.empa.ch

Impressum

Datum: 13. März 2006

Im Auftrag des Bundesamt für Energie, Forschungsprogramm Brennstoffzellen und Wasserstoff

Mühlestrasse 4, CH-3063 Ittigen

Postadresse: CH-3003 Bern

Tel. +41 31 322 56 11, Fax +41 31 323 25 00

www.bfe.admin.ch

BFE-Projektleiter: Andreas Gut, andreas.gut@bfe.admin.ch

Projektnummer: 100411

Bezugsort der Publikation: www.energieforschung.ch

Für den Inhalt und die Schlussfolgerungen ist ausschliesslich der Autor dieses Berichts verantwortlich.

Table of Content

Abstract 2
Resumé 2
1. Background 3
2. Aim and structure of the project 4
3. Results 4
3.1 Literature survey 4
3.2 Material synthesis 6
3.3 Minor element additions 8
3.4 Phase analysis of $BaZr_{1-x}Y_xO_{3-\delta}$ 9
3.5 Proton concentration 10
3.6 Conductivity 11
3.6.1 Experimental and data Interpretation 11
3.6.2 Influence of the yttria content on the conductivity 14
3.6.3 Influence of the powder synthesis method on the conductivity 15
3.6.4 Influence of minor element additions on the conductivity 15
3.6.5 Influence of high temperature sintering on the conductivity 16
3.7 Quasi-elastic neutron scattering 17
4. Discussion 18
5. Conclusions 19
References 21
Further publications from the project 21

Abstract

Solid oxide proton conductors can offer a new intermediate temperature fuel cell technology combining the advantages of polymeric fuel cells and solid oxide fuel cells. Among potential proton conductor materials, Y-doped barium zirconate (BZY) was found to be a promising candidate. This material was synthesised and characterised at Empa. The synthesis study shows the possibility to use up scalable methods to produce BZY. It was demonstrated that BZY can take up protons and that the protons are the mobile charge carriers that dominate the conductivity. The conductivity of the grain interior (log σ ~ -3 S.cm^{-1} at 300°C) competes with the conductivity of the best proton conductors. A correlation between the bulk conductivity and the cubic lattice parameter was observed. It was found that controlling the lattice parameter during the synthesis enable to tune the conductivity. The total conductivity of the test material was found to be dominated by the large resistive grain boundary contribution. Neither a clear microstructure/conductivity relationship could be identified nor could be found a blocking secondary phase. Only an exceptional thermal treatment (annealing up to 2200°C) showed an improvement of the grain boundary conductivity. A first interpretation presumes an electronic effect arising from the shearing of crystallographic planes that depresses either the proton concentration or the proton mobility in the vicinity of the grain boundaries (i.e. in the so called “space charge region”). Consequences for the further development of BZY for fuel cell application are discussed.

Resumé

Les oxydes conducteurs du proton ouvrent une nouvelle voie dans le développement de piles à combustible. Fonctionnant à des températures intermédiaires, ils peuvent allier les avantages des piles à combustible à électrolytes polymères et électrolytes oxydes. Parmi les matériaux potentiels, les zirconates de baryum dopé à l´yttrium (BZY) sont prometteurs. Ce matériau a été synthétisé et caractérisé à l´Empa. La synthèse peut être réalisée par des méthodes à grande échelle. Il a aussi été démontré que BZY incorpore des protons et que la diffusion des protons est à l´origine de la conductivité. La conductivité du grain (log σ ~ -3 S.cm^{-1} à 300°C) rivalise avec celle des meilleurs conducteurs du proton. Cependant, une corrélation entre le paramètre de maille et la conductivité a été observée. Contrôler le paramètre de maille pendant la synthèse permet d´ajuster la conductivité. La conductivité des échantillons testés est dominée largement par la contribution résistive des joints de grains. Aucune relation entre la microstructure et la conductivité n’a été identifiée et aucune seconde phase bloquante n´est visible dans les joints de grains. Seul un traitement thermique à très haute température (~ 2200°C) a permis d´améliorer la conductivité des joints de grain. L´interprétation préliminaire des résultats indique qu´un effet électronique provenant du cisaillement des plans cristallographiques réduit la concentration ou la mobilité des protons au voisinage des joints de grain (appelé « zone de charge d´espace »). Quelques propositions sont émises sur le développement futur de BZY pour des applications « pile à combustible ».

1. Background

Solid oxide proton conductors can offer a new intermediate temperature fuel cell technology. This technology can combine the advantages of polymeric fuel cells (high fuel utilisation without performance degradation) with those of high temperature SOFC systems (hydrocarbon fuel). The Proton Conducting Fuel Cell (PCFC) is particularly suited for small cells and operation on methanol or other hydrocarbons, which can be derived from both fossil and regenerative sources. The systems will operate in the temperature range of 300-700°C so that they offer both excellent thermal management strategies and good electrode kinetics, whilst still allowing relative ease of device fabrication for fuel cell and electro catalysis applications. Unfortunately, neither polymers nor solid oxide electrolytes are suitable for operation at such temperatures; however a less studied class of materials, ceramic proton conductors do typically exhibit good conduction properties at these temperatures, because at these temperatures they are in general more accelerated than oxygen ions. The fuel cell system can be seen as an intermediate step in the transition from fossil fuels to a regenerative, hydrogen oriented fuel economy.

The understanding of proton conductors is not easy and has apparently led to severe misinterpretation of the electrical properties. In consequence, this class of materials has inherited from a negative reputation of this materials class. Recent European research has been performed on the basic physical properties of proton conducting oxides and the development of new compositions and fabrication techniques to produce materials with improved properties. Most of the promising proton conductor electrolytes belong to the perovskite class of materials. Among these, $BaCe_{0.9}Y_{0.1}O_{3-\delta}$ turns out to have promising properties for direct internally reforming fuel cells based on hydrocarbon fuels [1]. However the chemical stability under operating conditions limits the use of this material. More stable are $BaZr_{1-x}Y_xO_{3-\delta}$ for which contradicting results regarding its proton conductivity are reported in the recent literature.

Besides the controversies regarding the electrical properties of these proton conductors, the ceramic processing to obtain performing electrolyte layers is a further crucial aspect in the development of PCFC.

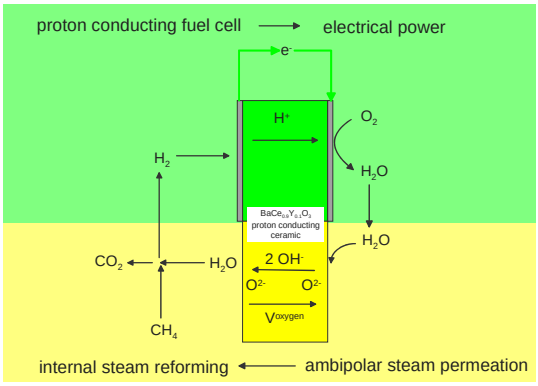


Figure 1 *Operating principle of a proton conducting fuel cell. In $BaCe_{0.9}Y_{0.1}O_{3-\delta}$, proton conductivity and steam permeation can occur independently. This allows for fuel cell operation and internal reforming making the system multifunctional on an atomic scale. The fuel cell device is therefore in principal able to be operated with dry hydrocarbons as fuels.*

2. Aim and structure of the project

The aim of the project was to identify suitable proton conducting ceramics, which can be used to fabricate dense and conductive electrolyte layers. It corresponds to the first step in demonstrating the proton conducting fuel cell concept.

First, perspectives and problems of $BaZr_{1-x}Y_xO_{3-\delta}$ have been surveyed in detail based on a literature review about proton conducting ceramics. The second step was the materials synthesis and characterisation with respect to the crystallographic and chemical properties. Standard ceramic processing was evaluated as well as potential up scalable routines. In the last part, the electrical performances of the various prepared materials have been investigated.

The framework of the project was a Ph.D. work (kick-off: Feb. 2004 – end: Feb. 2006). It was performed at Empa, Laboratory for High Performance Ceramics and supervised by Prof Dr. Ulrich Stimming, Physik-Department E19, Technische Universität München.

3. Results

3.1 LITERATURE SURVEY

Proton conductivity in simple perovskites (Table 1) has been demonstrated for the first time by Iwahara in 1981 [2]. The principle is based on partly substituting the host perovskite by undervalent ions in order to create the oxygen vacancies, which act as sites for the so called “protonic defects”. The protonic conductivity in hydrogen atmosphere is of the order of ~ 10^{-2} S/cm at 600°C.

In 1995, Nowick et al. proposed a new class of materials: the mixed or complex (as referred for the following) perovskites (Table 1) [3]. By taking the perovskites off cation stoichiometry, negative charges are created and are then compensated by oxygen vacancies. Here protons are not compensated by discrete localized charges like in simple perovskites, but by a statistical deviation of the number of B´ and B´´ ions from the stoichiometric values. This structure may prevent from trapping oxygen vacancies or protonic defects (that may happen in simple perovskite).

In recent time, the research for better proton conductors has lead to investigations of a large range of other oxide classes i.e. brownmillerite, pyrochlore (Table 1)...

From the extensive work of the past 20 years, $BaCe_{0.9}Y_{0.1}O_{3-\delta}$ (referred below as BCY10) for the simple perovskites and $Ba_3(Ca_{1.18}Nb_{1.82})O_{9-\delta}$ (referred below as BCN18) for the complex perovskites are considered as “classical” materials. Synthesised by solid-state reaction, pressed and sintered, they often serve as references. BCY10 and BCN18 show the best conductivity (~ 10^{-2} S/cm at 600°C) of proton conductors in their class of material.

Table 1 *Characteristics of proton conductors.*

	Doped perovskite and related structure				Fluorite related
	Simple perovskite	Complex or mixed perovskite		Brownmillerite	Pyrochlore
	$AB´_{1-x}B´´_xO_{3-\delta}$	$A_3B´_{1+x}B´´_{2-x}O_{9-\delta}$	$A_2B´_{1+x}B´´_{1-x}O_{6-\delta}$	$A_2B´_{1-x}B´´_xO_{5-\delta}$	$A_2B´_{2-x}B´´_xO_{7-\delta}$
Charge	A 2+	A 2+	A 2+	A 2+	A 3+
	B´ 4+	B´ 2+	B´ 3+	B´ 3+	B´ 4+
	B´´ 3+	B´´ 5+	B´´ 5+	B´´ 3+	B´´ 2+
Particularity	Trivalent dopant	Taken off stoichiometry		Ordering of oxygen	Smal activation energy
		B´ and B´´ ordering		vacancies	Open structure
		Trapping avoid			
Vacancies/x	$\delta = 1/2\ x$	$\delta = 3/2\ x$	$\delta = 1/2 + x$		

Although lots of different compounds have already been studied, combining high proton conductivity (that is to say above 10^{-2} S/cm) (Figure 2) and chemical, mechanical and thermodynamic stability remains a key problem for practical applications of proton conducting oxides in fuel cells. Alkaline earth cerates (e.g. $BaCeO_3$-based compounds) show high conductivity and low phase stability to carbonate or hydroxide formation, whereas alkaline earth zirconates (e.g. $BaZrO_3$-based compounds) are stable but show very low conductivity [4].

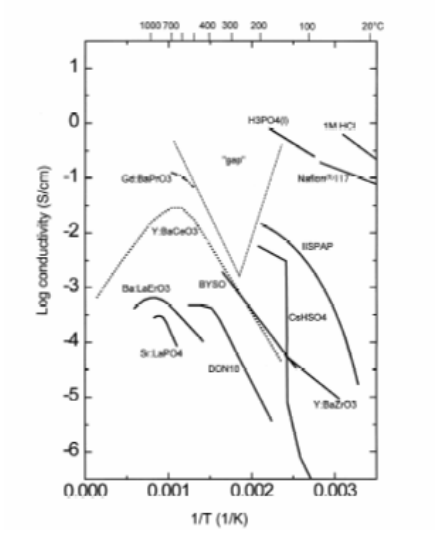


Figure 2 *Selected literature data from proton conductivity as a function of the inverse of the temperature (figure reproduced from [5]).*

$BaZrO_3$ is a well known material for its dielectric properties [6]. When doped with Y, $BaZrO_3$ becomes a proton conductor. It takes up water through oxygen vacancies, which are positively charged against the lattice and compensate the three valent yttria cations on the zirconia sites. It forms so-called “protonic defects” that are OH groups filling the vacant oxygen sites. For $BaZr_{0.9}Y_{0.1}O_{3-\delta}$ (referred below as BZY10) different water uptakes can be found in the literature (Figure 3**Fehler! Verweisquelle konnte nicht gefunden werden.**). The protonic defects as formed are free to move in BZY10.

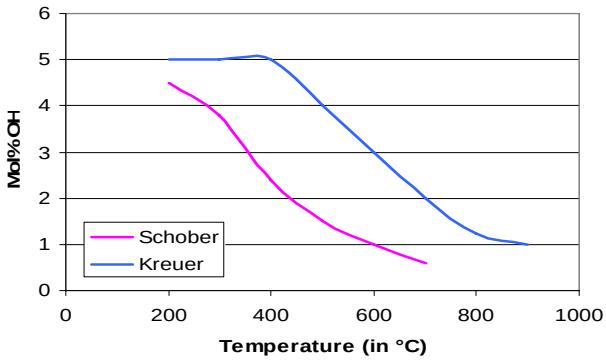


Figure 3 *Water uptake measured by Kreuer [7] and Schober [8] for BZY10.*

However BZY10 is known to be stable, but low conducting [4]. Recently, Kreuer et al. showed with thermodynamic and empirical arguments that $BaZr_{0.9}Y_{0.1}O_{3-\delta}$ (referred below as BZY10) should not only have a high thermodynamic stability but also a good proton conductivity [9]. These results have motivated further investigations on this material. In 2004, a study from Snijkers et al. highlighted the discrepancies in conductivity measurements for BZY10 (Figure 4) [10]. The reasons for these discrepancies are yet unclear. Often the preparation, processing, or ill-defined Ba-content (and the formation of BaO second phase) are made responsible [6].

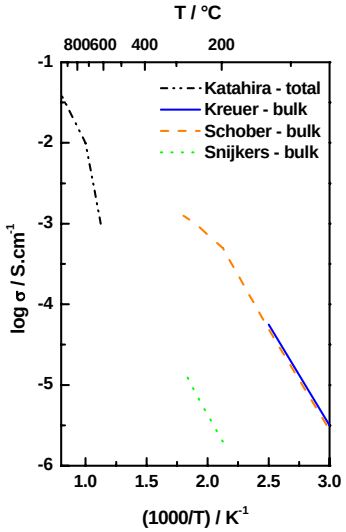


Figure 4 *Summary of impedance spectroscopy (IS) measurements for BZY10 [10].*

The literature review shows that BZY10 is a promising material for proton conducting fuel cells applications. Processing this material (synthesis and fabrication of dense layer) seems to be a crucial factor for the performance. The fabrication of the $BaZr_{1-x}Y_xO_{3-\delta}$ (with x=0, 5, 10, 15, 20) perovskites by different synthesis techniques and the further characterisation as regards the electrical conductivity is the main focus of this project.

3.2 MATERIAL SYNTHESIS

$BaZr_{0.9}Y_{0.1}O_{3-\delta}$ powder was synthesized by three different methods: solid-state reaction, spray pyrolysis and spray drying. The as synthesized powders have been milled, pressed and sintered to form dense pellets. The flow chart of the materials synthesis and the further preparation steps to obtain dense electrolytes are illustrated in Figure 5.

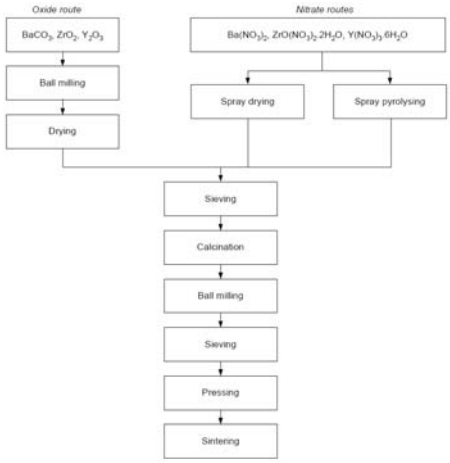


Figure 5 *Method of synthesis: solid-state reaction, spray pyrolysis and spray drying.*

The spray drying method is of particular interest as it leads to a low calcination temperature (~ 800°C). For the spray pyrolysis method, the citrates, used as ignitors, are decomposed during the atomisation and produce carbonated species, which are only decomposed at ~ 1200°C.

The different preparation methods lead to samples with different morphologies. The microstructure of a fracture cross section of the sintered specimens at 1500°C and 1720°C is shown in Figure 6. An important grain growth and a steadily diminishing porosity are observed when the sintering temperature is increased up to 1720°C (Figure 6-a2, a3) for the powder prepared by the solid-state reaction. The pellets reach about 94% of the theoretical density. For the spray pyrolysis and the spray drying methods, an improvement of the density is also observed with an increasing sintering temperature. A limited grain growth as well as an important increase in the pore size occurs for the spray pyrolysis method (Figure 6-c2, c3). Before the start of the densification, the grains of the spray dried powder calcined at 1200°C already reached their definitive size, no further grain growth occurs during sintering (Figure 6-b2, b3). The specimens prepared by the solid-state reaction method sintered at 1720°C and by the spray pyrolysis sintered at 1500°C and 1720°C show a good intergranular connectivity as for the other specimens the intergranular connectivity is low and the specimens are very fragile.

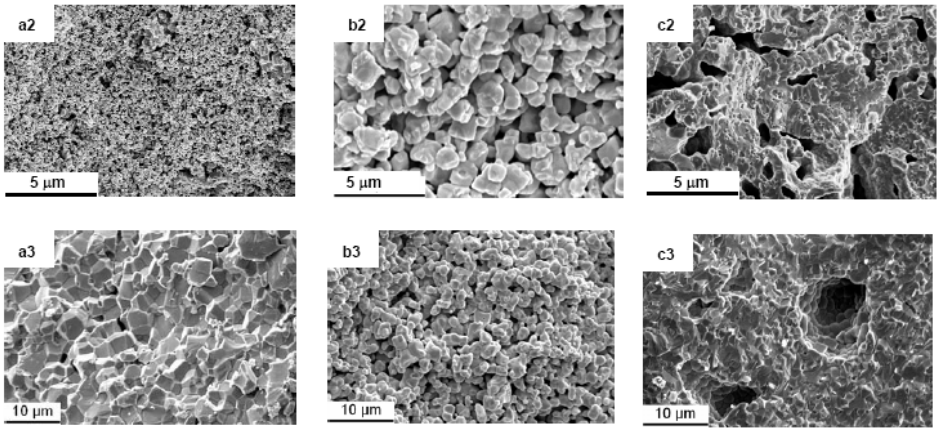


Figure 6 *Fracture cross section of sintered samples at 1500°C and 1720°C, respectively for the solid-state reaction method (a2 and a3), the spray drying (b2 and b3) and the spray pyrolysis (c2 and c3) methods.*

3.3 Minor element additions

As indicated from Figure 6, the densification of BZY10 is achieved only at high temperatures. In order to optimise the sintering and densification so called “sintering aids” additional elements in up to a few percentage quantity are often used in ceramic processing to overcome this problem.

Unless sintering aids are frequently used in the ceramic processing in order to densify materials at low temperature, very few works have been already carried out on BZY10 [11, 12]. Of potential sintering aids, a previous study of Al_2O_3, MgO, and Y_2O_3 showed a marginal improvement in the sintering behaviour [12]. An initial screening of the transition elements in the series Sc to Zn showed that NiO, CuO and ZnO are the most effective additives for enhancing barium zirconate densification [11]. In opposition V, Cr, and Fe worsened the densification behaviour. Moreover samples having additions of NiO and CuO changed colour (from white to black) after sintering. This latter feature may indicate a change in the conduction behaviour from ionic to electronic-type.

Several additives, presented in Table 2, were blended in the BZY10 powder by ball milling. Pellets were pressed and sintered at 1500°C for 10 hours or at 1720°C for 24 hours.

Table 2 *List of the different additives and their concentration.*

N°	Additive	Amount		
1	$BaCe_{0.9}Y_{0.1}O_{3-\alpha}$	1 mol.%		
2	$BaMo_{0.33}Y_{0.67}O_3$ (oxides precursors)	1 mol.%	4 mol.%	10 mol.%
3	$BaMoO_4$	1 mol.%		
4	MoO_3	1 mol.%	4 mol.%	
5	Mo	0.28 mol.% (0.1 w.%)		
6	$MgAl_2O_4$ (oxides precursors)	1. mol.%	4 mol.%	
7	$MgAl_2O_4$ (calcined at 1200 °C for 2 H)		4 mol.%	
8	SiO_2	1 mol.%		
9	TiO_2	1 mol.%		
10	MgO	0.05 mol.%	1 mol.%	2 mol.% (~0.3 w.%)
11	$La(OH)_3$	0.7 mol. % (0.2 w.%)		
12	Al_2O_3		4 mol.%	
13	Al-phosphate (AlO_4P)	0.23 mol. % (0.1 w.%)		
14	B-phosphate (BO_4P)	0.26 mol. % (0.1 w.%)		
15	$Ba_2Zr_{0.8}Y_{0.2}O_4$			
16	$BaZr_{0.89}Y_{0.1}Mg_{0.01}O_3$			
17	$Ba(NO_3)_2$	1 mol.%		10 mol.%

The following trends have been identified as regards the densification (see also Figure 7):

- is worsened using $BaMo_{0.33}Y_{0.67}O_3$ (1 mol.%), $BaMoO_4$ (1 mol.%), Mo (0.1 w.%), AlO_4P (0.1 w.%) and $Ba(NO_3)_2$ (1 mol.%),
- does not change using MoO_3 (1 mol.% and 4 mol.%), $MgAl_2O_4$ (1 mol.% and 4 mol.%), $MgAl_2O_4$ calcined (4 mol.%), SiO_2 (1 mol.%), TiO_2 (1 mol.%), MgO (0.05 mol.%), $La(OH)_3$ (0.2 w.%), $Ba_2Zr_{0.8}Y_{0.2}O_3$, and $Ba(NO_3)_2$ (10 mol.%),
- improves of about 15 % using $BaCe_{0.9}Y_{0.1}O_{3-a}$ (1 mol.%), $BaMo_{0.33}Y_{0.67}O_3$ (10 mol.%), MgO (2 mol.%), and Al_2O_3 (4 mol.%).

The density of BZY10 increases when the concentration of $BaMo_{0.33}Y_{0.67}O_{3-\alpha}$, MgO, and $Ba(NO_3)_2$ increases. On the contrary, the densification of BZY10 decreases when the concentration of MoO_3 and $MgAl_2O_4$ increases.

Among the additives tested in the present work, the denser samples are obtained by using $BaCe_{0.9}Y_{0.1}O_{3-\alpha}$ (1 mol.%), $Ba(NO_3)_2$ (10 mol.%) and MgO (2 mol.%) and have around 80% of the theoretical density. This value is still far from a target value of 98% density, required for application as a solid electrolyte.

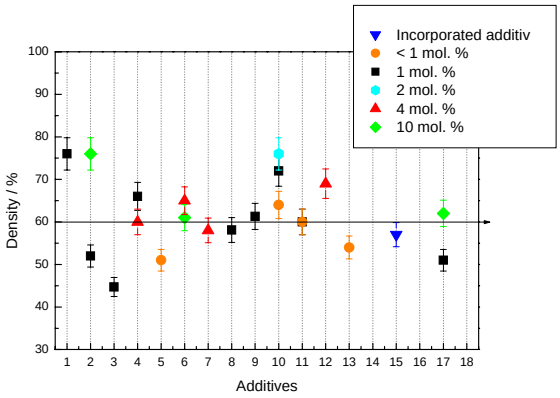


Figure 7 *Percentage of the theoretical density (6.2 g/cm^3) [10] obtained after sintering at 1500°C for 10 hours using the additives 1 to 17, as named above, in different concentrations.*

3.4 PHASE ANALYSIS OF $BaZr_{1-x}Y_xO_{3-\delta}$

The phase and the structure of $BaZr_{1-x}Y_xO_{3-\delta}$ were analysed by x-ray diffraction (XRD). Figure 8**Fehler! Verweisquelle konnte nicht gefunden werden.** shows the resulting lattice parameter of BZYx for different yttria contents x (x=0, 5, 10, 15, 20). After calcination at 1200°C, the lattice is found to be cubic and within the experimental error the lattice parameter is surprisingly independent on the Y content. After sintering above 1500°C, the lattice parameter remains cubic and is found to increase linearly with the Y content.

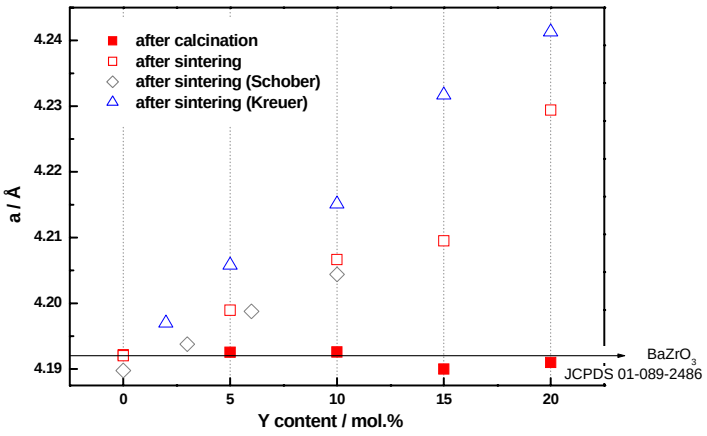


Figure 8 *Lattice parameter of BZYx after calcinations at 1200°C and 1400°C for 10 hours and after sintering as a function of the dopant level. The results are compared to values from the literature. Schober et al. [8] and Kreuer et al. [7] find a cubic lattice parameter for x=0 and 5. For x≥10, Kreuer et al. find a tetragonal structure.*

BZY10 prepared by the different methods and sintered at 1500°C or at 1720°C were found to have one cubic structure except the specimen prepared by the solid-state reaction method and sintered at 1500°C (Table 3). This sample presents an additional BZY10 phase, which was found to be tetragonal. The lattice parameters of the samples prepared by the nitrate routes are significantly smaller (0.4197 nm) than the one (0.4206 nm) of the sample prepared by the solid-state reaction method and sintered at 1720°C.

All additives decrease the lattice parameter up to 0.4182 nm for TiO_2 (Table 3).

Table 3 *Lattice parameter of the sintered pellets prepared by the different synthesis methods and with some additives.*

Method	Thermal history		a=b=c (nm)	V_{cell}, a^3 (m^3)
	Calcination (T/°C-t/h)	Sintering (T/°C-t/h)		
Solid-state reaction	1200-10 + 1400-10	1500-10	0.4192 + a=b=0.4202 c=0.4220	73.66×10^{-30} 74.58×10^{-30}
		1720-24	0.4206	74.34×10^{-30}
with Al_2O_3 (4 mol.%)			0.4198	73.99×10^{-30}
with MgO (1 mol.%)			0.4200	74.10×10^{-30}
with TiO_2 (1 mol.%)			0.4182	73.13×10^{-30}
with Mo (0.3 mol.%)			0.4199	74.03×10^{-30}
With Bi_2O_3 (1 mol.%)			0.4205	74.30×10^{-30}
Spray pyrolysis	1200-10	1500-10	0.4202	74.20×10^{-30}
		1720-24	0.4192	73.65×10^{-30}
Spray drying	1200-10	1500-10	0.4196	73.88×10^{-30}
		1720-24	0.4197	73.95×10^{-30}

3.5 PROTON CONCENTRATION

In order to investigate to which extend BZY is saturated with protons, the samples are humidified at 600°C. Under these wet atmospheres, the materials should be in thermodynamic equilibrium with the surrounding atmosphere. They were subsequently quenched by removing them quickly from the furnace and weighed with a precision scale. The concentration of proton was determined by the weight changes. Figure 9 presents the proton concentration versus the Y content in comparison with the theoretical proton content. As expected the proton content is a function of the Y content. By doubling the Y content, the proton defect concentration is also doubled. However, the theoretically possible proton concentration was not reached, which implies that not all vacancies could be filled.

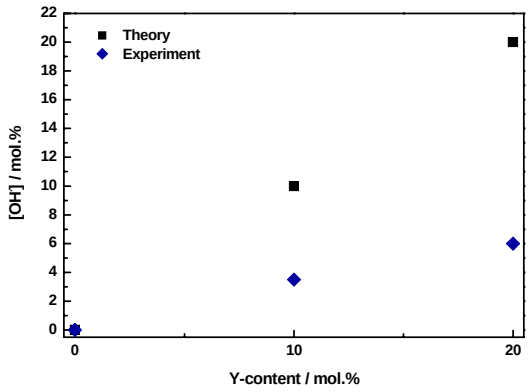


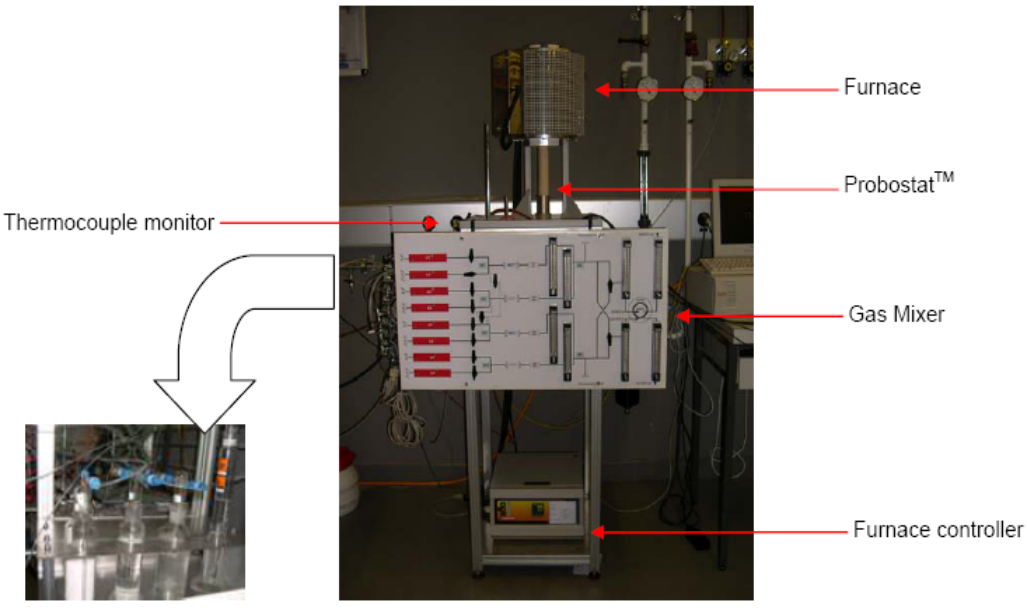
Figure 9 *The proton content at 600°C in wet oxygen is represented as a function of the Y substitution content. For comparison purpose, the theoretical proton content is added.*

3.6 CONDUCTIVITY

3.6.1 Experimental and data Interpretation

In order to test the electrical conductivity of proton conducting materials, the test set-up has to be able the perform tests under controlled temperature, oxygen and water pressures. A special test set-up has been designed and built up during this project (Figure 10**Fehler! Verweisquelle konnte nicht gefunden werden.**).
The setting is composed of a Probostat™, a furnace and a gas mixer. The Probostat™ is a cell for measurements of:

- electrical properties (DC, AC, impedance spectroscopy),
- dielectrical properties,
- ionic (oxygen ion, proton) conductivity and transport number,
- I,V characteristics,
- electrochemical pumping, gas permeation and electro catalysis.



Drying – wetting station

Figure 10 *Set-up for characterising proton conducting ceramics.*

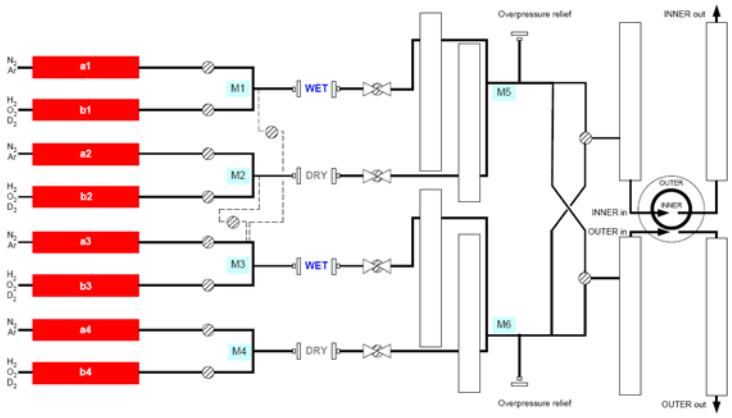


Figure 11 *Flow chart of the gas mixer.*

The furnace, a vertical tubular furnace, which covers the closed outer tube of the Probostat^{TM}, sets the temperature around the sample. The sample position is located in the centre of the hot zone of the furnace.

The gas mixer (Figure 11**Fehler! Verweisquelle konnte nicht gefunden werden.**) has been designed for controlling the atmospheres in one or two chambers. Variable partial pressure of oxygen, hydrogen or deuterium can be set independently of the partial pressure of water. The gas mixer is build up with mass flow controllers controlled by a computer, and gas wash bottles containing a drying agent (P_2O_5), or distilled water, or distilled water with KBr Specifications of the test rig are summarised in Table 4.

Table 4 *Measurement range.*

Parameter	Working range
Total flow rate	2.5 to 250 ml/min
Partial pressure of water	3 10^{-4} to 22 hPa

Gas mixing	O_2 _ Ar (or N_2) (2 10^{-7} _ 1 bar) H_2 _ Ar (or N_2) (1 10^{-7} _ 1 bar) D_2 _ Ar (or N_2) (1 10^{-7} _ 1 bar)

Impedance spectroscopy was performed under dry and wet gas atmospheres by using a Solartron 1260 Frequency Response Analyser. The impedance was analysed by using models based on electrical equivalent circuits to separate grain boundary and bulk conductivities in the various gas atmospheres.

Typical impedance spectra are given in Figure 12. The impedance spectra represent bode Z´-Z´´ plots for the different preparation methods. At 300°C, one or two processes depending on the preparation method can be clearly identified. Based on the order of magnitude of the values for the specific capacitances of the high and the low frequency semicircles (~ pF.cm^{-1} (C_b) and ~ nF.cm^{-1} (C_{GB}) respectively), the corresponding resistances can be assigned to the bulk (i.e. grain interior) (R_b) and to the grain boundary (R_{GB}), respectively. The resulting overall equivalent circuit is described as (R_bC_b)($R_{GB}C_{GB}$). Following the temperature dependence of the impedance, bulk and grain boundary contributions could be separated for all materials investigated.

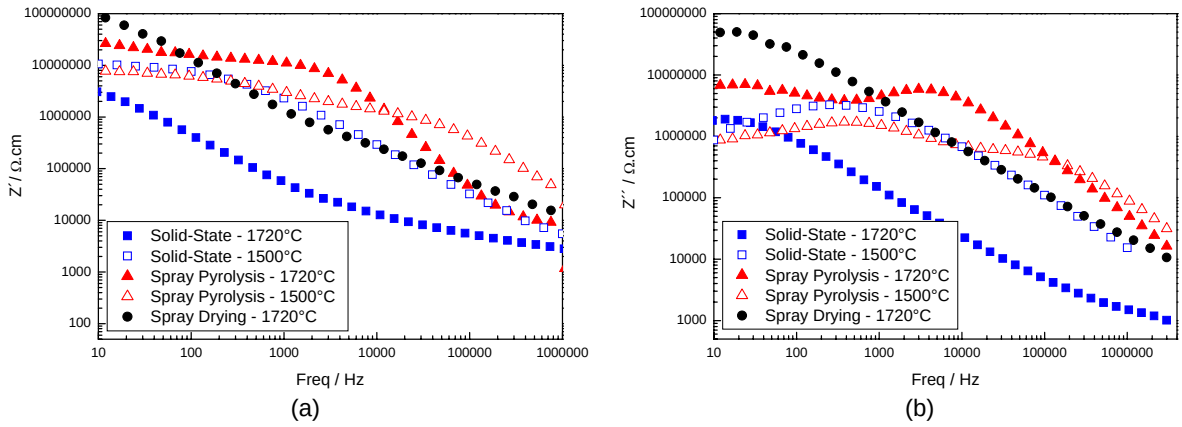


Figure 12 *Impedance spectra of the real part (a) and of the imaginary part (b) for BZY10 for different synthesis methods.*

The bulk and the grain boundary conductivity, as interpreted above, are compared to the literature values in Figure 13. The bulk conductivity is slightly lower than reported by Schober et al. [13] and Kreuer et al. [7], but about one order of magnitude higher than reported by Snijkers [10]. It indicates that the bulk conductivity is highly dependent on the measuring conditions as well as on the preparation method. The grain boundary conductivity is much lower than the bulk conductivity and is the dominating contribution. In accordance with others e.g. the work from Katahira [14], which also identify the grain boundary conductivity as the limiting contribution.

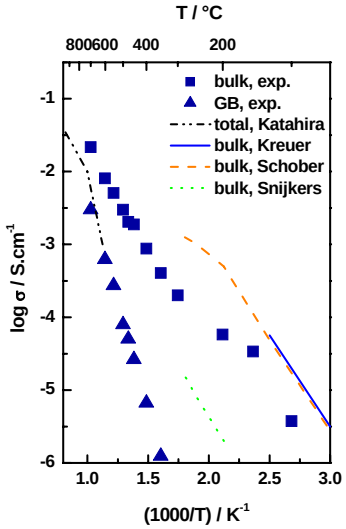


Figure 13 *The temperature dependence of the conductivity of the bulk and the grain boundary of BZY10 prepared by the solid-state reaction method at Empa are compared with the literature values from Schober [13], Kreuer [7], Katahira [14], and Snijkers [10].*

3.6.2 Influence of the yttria content on the conductivity

The dependence of the yttria content on the conductivity was investigated as a function of temperature in wet and dry atmospheres (Figure 14). Under wet conditions, the bulk conductivity of BZY20 is about one order of magnitude higher than the one of BZY10. In addition, the bulk conductivity for both BZY10 and BZY20 is much higher under wet conditions than dry ones. This indicates that protons are most likely the mobile charge carriers in these materials. The results are in agreement with the theory: the introduction of 1 Y cation creates 0.5 vacancies and after humidification 1 protonic defect (for keeping the electroneutrality of the materials).
For the grain boundaries, a similar trend is observed, however not as pronounced as for the bulk conductivity. Comparing the bulk and grain boundary conductivity, the grain boundary transport is the limiting transport in all $BaZr_{1-x}Y_xO_{3-\delta}$ proton conductors investigated.

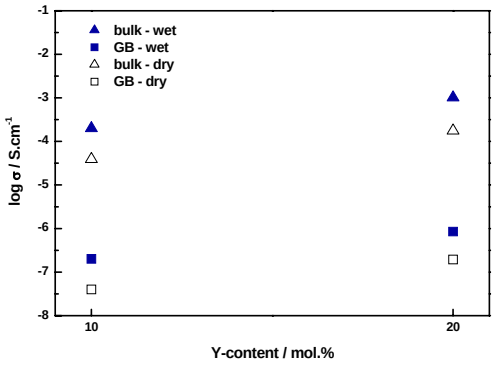


Figure 14 *Conductivity of the bulk and the grain boundary of BZY10 and BZY20 in wet and dry oxygen at 300°C.*

3.6.3 Influence of the powder synthesis method on the conductivity

The different synthesis methods applied in this study resulted in cubic perovskite type $BaZr_{1-x}Y_xO_{3-\delta}$ but showed small differences in the lattice parameters (Table 3). The influence of the preparation procedure on the conductivity and microstructure has been in detailed described in [15].
As can be seen in Figure 15, a tendency is that the bulk conductivity increases for larger lattices. Even these small changes in the lattice parameter correspond to an increase of three orders of magnitude in the conductivity.

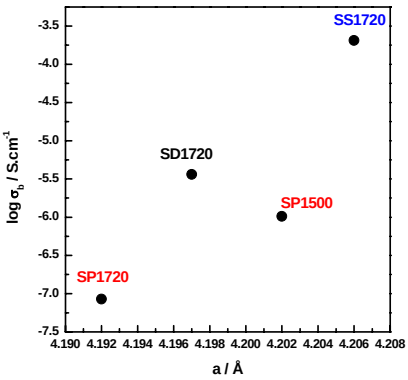


Figure 15 *Bulk conductivity at 300°C under wet oxygen is plotted as a function of the lattice parameter.SP1500 and SP1720 refer to spray pyrolised BZY10 sintered at 1500°C and 1720°C, respectively. SD1720 and SS1720 refer to BZY10 sintered at 1720°C and produced by spray drying and solid state reaction, respectively.*

As regards the pronounced grain boundary resistance, no clear correlation between the microstructure, density and the grain boundary conductivity could be observed. This indicates that the sintering and resulting bonding between the BZY10 particles is most probably not an important factor that limits the grain boundary conductivity. Furthermore, SEM investigations around the grain boundaries did not reveal any hint for a second phase formation, which could have explained the high grain boundary resistivity.

3.6.4 Influence of minor element additions on the conductivity

Adding metal ions to BZY10 lowers:

- the lattice parameter
- the bulk and grain boundary conductivity compared to the “pure” BZY10.

Similarly to the specimens prepared by different routes, the lattices containing additives show a striking dependence of the bulk conductivity with conductivity (Figure 16). Specimens with large lattices present the highest conductivities.

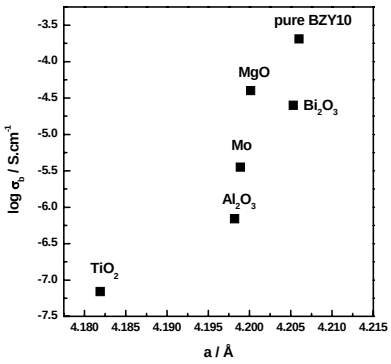


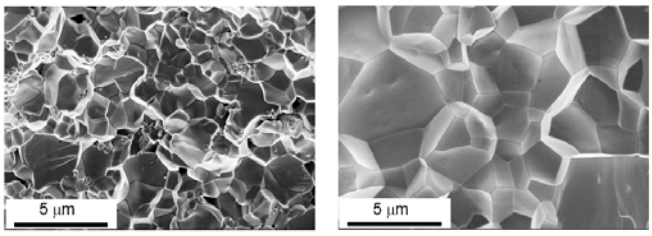
Figure 16 *Bulk conductivity at 300°C under wet oxygen is plotted as a function of the lattice parameter.*

3.6.5 Influence of high temperature sintering on the conductivity

In order to minimise the persisting grain boundary contribution, a further attempt was made to diminish the amount of grain boundaries by a thermal treatment at ~ 2200°C in an optical floating zone furnace (common technique used to grow single crystals) at the Paul Scherrer Institute. In the case of BZY, this technique turned out to be not applicable to grow single crystals due to the higher melting temperature of BZY.

The sample preparation started from $BaZr_{0.9}Y_{0.1}O_{3-\delta}$ powder prepared by the solid-state reaction method described in paragraph “Materials synthesis”. The powder was then isostatically pressed into a rod (8 cm long, 6 mm diameter). The sample was sintered and annealed in two subsequent steps:

- in a chamber furnace at 1720°C for 24 hours in a powder bed of already sintered BZY10 powder. The sample as sintered will be named SB-sample hereinafter,
- in the optical floating zone furnace (FZ-T-10000-H-IV-VP-PC, Crystal System Corp., Japan) using four 1000 W halogen lamps as a heat source. The focused light was moved along the rod (up and down) with a rate of 5 mm/h. The maximum temperature in the heating zone was about 2200°C. The atmosphere was set to 2 bar with 240 ml/min Ar and 12 ml/min O_2 flowing. The sample as further heat treated in the optical floating zone furnace will be named FZ-sample hereinafter.



(a) (b)

Figure 17 *Fracture cross section of the SB-sample (a) and the FZ-sample (b).*

The resulting BZY10 FZ-sample, shows the following properties (for details see [16]):

- the same phase and lattice parameter than the SB-sample, sintered at 1720 °C,
- bigger grains and a more homogenous microstructure with less grain boundaries than the SB-sample (Figure 17),
- the same bulk conductivity than the SB-sample (~10^{-3} S/cm at 400°C) (Figure 18),
- an activation of the bulk in wet conditions comparable to values published in the literature [13, 17] and corresponding to proton conduction
- an activation of the grain boundary in wet conditions, which is becoming closer to characteristics values of proton conduction (Table 5),
- an activation energy, which turns non protonic in dry conditions,
- the grain boundary conductivity about 2 orders of magnitude higher than for the SB-sample.

The important feature of the high temperature annealing is the increase in the grain boundary conductivity of about two orders of magnitude, while the bulk conductivity remains unaffected. The differences in the microstructure were taken into account by correcting the grain boundary contribution for the differences in grain sizes as suggested by Haile et al. [18]. The result is given in Figure 18. The correction has only a minor impact on the measured data and thus does not explain the observed improvement in the grain boundary conductivity.

No indication for a second phase formation in the vicinity of the grain boundaries was observed neither for specimen prepared by conventional sintering nor after the high temperature treatment in the floating zone furnace. Therefore second phase formation was ruled out as a reason for the observed improvement.

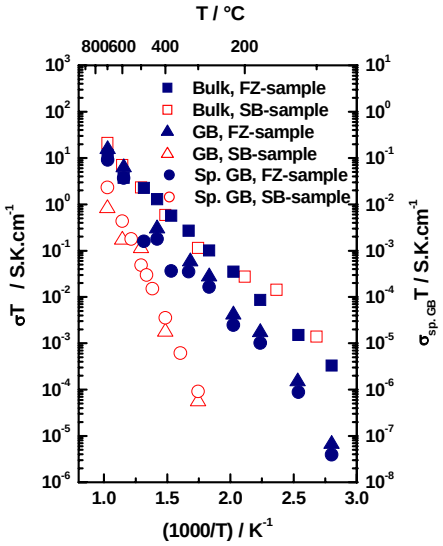


Figure 18 *The conductivity of the bulk and the apparent and specific grain boundary for FZ- and SB-samples, measured in water saturated oxygen. The data are presented as an Arrhenius plot. The specific grain-boundaries take into account the microstructure.*

Table 5 *Comparison of the activation energy and the pre-exponential factor of the bulk and the grain boundary of the SB- and FZ-samples in water saturated oxygen and dry oxygen below 300°C.*

	$E_{a\ FZ}$ (eV)	$E_{a\ SB}$ (eV)	$\sigma_{0\ FZ}$ (KS/cm)	$\sigma_{0\ SB}$ (KS/cm)
		WET O_2 pH_2O=22 hPa		
Bulk	0.49	0.42	$4.4*10^3$	$1.1*10^3$
Grain boundary	0.55	1.2	$8.1*10^3$	$4.6*10^6$
		DRY O_2 $pH_2O=10^{-4}$ hPa		
Bulk	0.8	0.53	$9.5*10^5$	$2.1*10^3$
Grain boundary	0.9	1.3	$4.9*10^5$	$2.9*10^6$

3.7 QUASI-ELASTIC NEUTRON SCATTERING

The separation of the different contributions (bulk and grain boundaries) to the conductivity was done based on equivalent circuit modelling of impedance data. Even though this approach is well accepted in the scientific community, an independent verification is of course advantageous. Quasi elastic neutron scattering (QENS) gives a direct access to the chemical diffusivity of protons, D. Knowing the proton concentration, the impedance data can be used to calculate back the diffusivity of BZY10 and can be compared to the neutron scattering data.

For the quasi elastic neutron scattering experiment BZY10 was loaded at 600°C for 24 hours with protons in humid atmosphere in order to reach ~3.0 mol.% of protonic defects. For impedance measurements, the same amount of protons was also loaded.

The result is shown in Figure 19. They clearly confirm high bulk proton conductivity for BZY10. The QENS measurement shows the highest proton mobility. Significant lower values are calculated for impedance spectroscopy data. A similar difference between both techniques was observed earlier in the literature for BZY15 [19]. On a first view the agreement between the diffusivity obtained by QENS and by IS seems to be really poor. The diffusivity measured by QENS reveals more than 100 times faster proton transport phenomena than observed by IS. However, IS evaluates an effective diffusion coefficient, whereas QENS detects a chemical one. IS is not able to determine such fast processes like strongly localized motions of the protons but only translational long time jump diffusion.

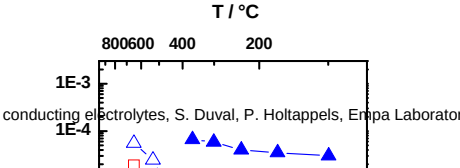


Figure 19 *Comparison of data obtained by neutron scattering and by impedance spectroscopy (IS) for BZY10.The values are compared to literature values from Hempelmann et al. [19] for BZY15.*

4. Discussion

A significant variation of the lattice parameter is observed for the different processing conditions (method and sintering temperature) and addition of impurities. It might arise from:
1) yttria is not built in into the lattice,
2) Ba deficient perovskite due to Ba-evaporation during the sintering or barium carbonate formation,
3) lattice distortions or appearance of several phases simultaneously, which are beyond the detection level in our XRD diffractograms [7, 20].

A striking dependence of the lattice parameter on the activation energy is found for all samples as summarized in Figure 20. The larger lattice parameters were found to correspond to the smaller activation energies. Big, polarisable cations and wide lattices provide powerful oxygen dynamics, while small cations and dense, stiff oxygen sublattices do not. Protons spend most of the time rotating with very low activation energy around their host oxygen ion, forming weak temporary hydrogen bonds to the neighbouring oxygen. Only rarely it does actually jump to that neighbouring oxygen ion.

Therefore, the results from this work favour the interpretation according to which the different activation energies/lattice parameters of BZY10 arise from the occurrence of two polymorphs. The one with a low conductivity and a small unit cell volume, i.e. the α-phase, is thermodynamically stable, and the fast conductive phase, i.e. the β-phase, has a larger unit cell volume and is presumed to be metastable [21]. The large unit cell seems to originate from a limited cross-site substitution and lead to restricted defect associations. Consequently, this β-phase should have lower activation energy. The combined decrease in defect association and lattice expansion increase the protonic conductivity as is observed in our experiments.

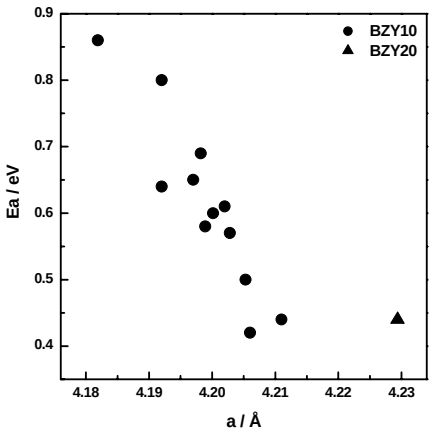


Figure 20 *Activation energy of the differently prepared specimen as a function of the lattice parameter.*

The most prominent limitation in the proton conductivity in BZY10 is clearly identified to be the grain boundary. To understand the physical nature of this limitation is the most important aspect in the further development of proton conducting electrolytes.

In this work, different microstructures and element additions have been investigated. Neither a clear microstructure/conductivity relationship could be identified, nor blocking (or as well better conducting) secondary phases could be found using SEM. Only an exceptional thermal treatment (annealing up to 2200°C) showed an improvement of the grain boundary conductivity.

The nature of grain boundaries and their impact on the conductivity was discussed by Kim et al. [22] and Fleig et al. [23]. The "simplest" grain boundary can be considered a dislocation of crystallographic planes. The possible impact on the electronic structure and charge carrier concentration is illustrated in Figure 21. Since no indications for second phase formation is observed, an electronic effect following one of these possibilities is suggested to explain the nature of the large grain boundary resistance.

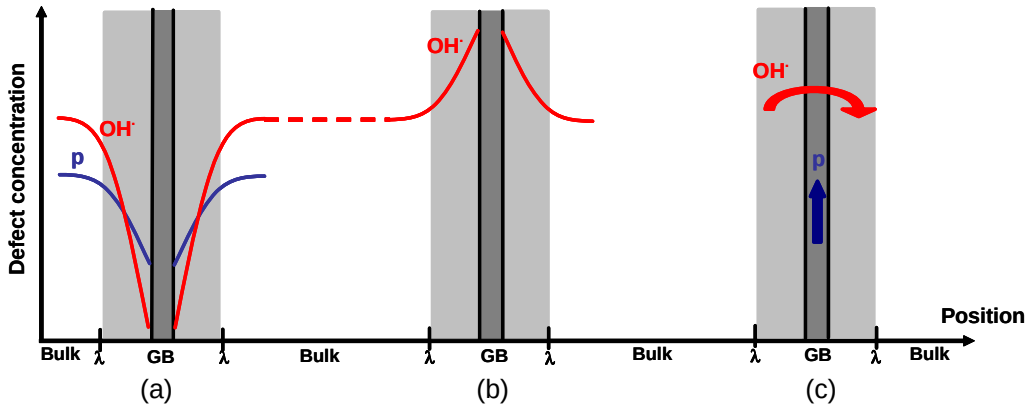


Figure 21 *Space charge model for grain boundary: charge carrier depletion in the space charge zone (a), charge carrier increase in the space charge zone (b), two pathways for conductions: ionic along the grains and electronic in the grain boundaries (c).*

5. Conclusions

The development of ceramic proton conducting electrolytes is still a challenge. The requirements during fuel cell fabrication and operation on stability and conductivity rule out several highly conductive materials for this application. Based on a literature review, $BaZr_{0.9}Y_{0.1}O_{3-\delta}$ was selected because of its

stability and predicted relatively high proton conductivity. The results from conductivity and quasi-elastic neutron scattering have confirmed high bulk proton conductivity in this material. However, overcoming the grain boundary resistance is still THE persisting problem for implementing this material into ceramic fuel cells.

In order to control the bulk conductivity the occurrence of the conductive phase of BZY10 has to be monitored during the preparation of the specimens.

In order to enhance the grain boundary conductivity, the materials synthesis, and the heat treatment during sintering, as well as “doping” the materials with other elements were investigated. From these efforts, only the high temperature annealing of the proton conductor led to a significant improvement of the grain boundary conductivity. Changes in the crystallography due to heat treatment or additions also affect the bulk conductivity, but the trends are still not conclusive and the analysis is ongoing. As regards the grain boundary resistance, no indications for a formation of a second, severe blocking phase in the grain boundaries were obtained. Therefore, the resistance of the grain boundaries is interpreted to be of electronic nature, e.g. a positive charge arising from dislocation of crystallographic planes that can depress and immobilise the protons in a so called “space charge region”. Such intrinsic crystallographic failures are likely to be overcome by extreme heat treatment (as we did). But also a controlled growth of thin films could be promising. The latter option opens a new area of activity, which is beyond the scope of this project.

Beyond the fuel application, the electrical properties of BZY might be interesting for sensor applications. This would include classical concepts (e.g. potentiometric sensors based on the Nernst potential), but also the grain boundaries could be interesting, by being sensitive to other elements, affecting the electronic structure and therefore the conductivity through the sample (amperometric sensors).

References

[1] Coors W. Grover: Protonic ceramic fuel cells for high-efficiency operation with methane, J. Power Sources, 2003, 118, 1-2, 150-156.

[2] Iwahara Hiroyasu, Esaka T., Uchida H. and Maeda N.: Proton conduction in sintered oxides and its application to steam electrolysis for hydrogen production, Solid State Ionics, 1981, 3-4, 359-363.

[3] Nowick Arthur S. and Du Yang: High-temperature protonic conductors with perovskite-related structures, Solid State Ionics, 1995, 77, 137-146.

[4] Iwahara Hiroyasu, Yajima T., Hibino T., Ozaki K. and Suzuki H.: Protonic conduction in calcium, strontium and barium zirconates, Solid State Ionics, 1993, 61, 65-69.

[5] Norby Truls: Solid-state protonic conductors: principles, properties, progress and prospects, Solid State Ionics, 1999, 125, 1-11.

[6] Ubaldini Alberto, Buscaglia Vincenzo, Uliana Claudio, Costa Giorgio and Ferretti Maurizio: Kinetics and mechanism of formation of barium zirconate from barium carbonate and zirconia powders, J. Am. Ceram. Soc., 2003, 86, 1, 19-25.

[7] Kreuer Klaus-Dieter, Adams St., Munch W., Fuchs A., et al.: Proton conducting alkaline earth zirconates and titanates for high drain electrochemical applications, Solid State Ionics, 2001, 145, 1-4, 295-306.

[8] Schober Tilman and Bohn H. G.: Water vapor solubility and electrochemical characterization of the high temperature proton conductor BaZr0.9Y0.1O2.95, Solid State Ionics, 2000, 127, 3-4, 351-360.

[9] Kreuer Klaus-Dieter: Aspects of the formation and the mobility of protonic charge carriers and the stability of perovskite-type oxides, Solid State Ionics, 1999, 125, 285-302.

[10] Snijkers Frans M. M., Buekenhoudt Anita, Cooymans Jos and Luyten Jan J.: Proton conductivity and phase composition in BaZr0.9Y0.1O3-[delta], Scripta Mater., 2004, 50, 5, 655-659.

[11] Babilo Peter and Haile Sossina M.: Enhanced sintering of yttrium-doped barium zirconate by addition of ZnO, J. Am. Ceram. Soc., 2005, 88, 9, 2362-2368.

[12] Azad Abdul-Majeed, Subramaniam Selvarajan and Dung Teng Wan: On the development of high density barium metazirconate (BaZrO3) ceramics, J. Alloy Compd., 2002, 334, 1-2, 118-130.

[13] Bohn Hans G. and Schober T.: Electrical conductivity of the high-temperature proton conductor BaZr0.9Y0.1O2.95, J. Am. Ceram. Soc., 2000, 83, 4, 768-772.

[14] Katahira Koji, Kohchi Yoshirou, Shimura Tetsuo and Iwahara Hiroyasu: Protonic conduction in Zr-substituted BaCeO3, Solid State Ionics, 2000, 138, 1-2, 91-98.

[15] Duval Sophie, Vogt Ulrich, Holtappels Peter, Stimming Ulrich and Graule Thomas: Characterisation of BaZr0.9Y0.1O3-a proton conductor prepared by three different synthesis methods: study of the sinterability and the conductivity, intended to be submitted to J. Electrochem. Soc..

[16] Duval Sophie, Holtappels Peter, Vogt Ulrich, Pomjakushina Ekatherina, et al.: Electrical conductivity of the proton conductor BaZr0.9Y0.1O3-a obtained by high temperature annealing, Solid State Ionics, accepted for publication.

[17] Münch W., Kreuer Klaus-Dieter, Seifert G. and Maier Joachim: Proton diffusion in perovskites: comparison between BaCeO3, BaZrO3, SrTiO3, and CaTiO3 using quantum molecular dynamics, Solid State Ionics, 2000, 136-137, 183-189.

[18] Haile Sossina M. and West David L.: The role of microstructure and processing on the proton conducting properties of gadolinium-doped barium cerate, J. Mater. Res., 1998, 13, 6, 1576-1595.

[19] Gross B., Beck Ch., Meyer F., Krajewski Th., et al.: BaZr0.85Me0.15O2.925 (Me=Y, In and Ga): crystal growth, high-resolution transmission electron microscopy, high-temperature X-ray diffraction and neutron scattering experiments, Solid State Ionics, 2001, 145, 1-4, 325-331.

[20] Kruth Angela, Mather Glenn C., Jurado Jose Ramon and Irvine John T.S.: Anomalous variations of unit cell parameters with composition in proton conducting, ACeO3-type perovskite solid solutions, Solid State Ionics, 2005, 176, 7-8, 703-712.

[21] Azad Abul, Savaniu Christian, Tao Shanwen, Duval Sophie, et al.: On the structural origins of the differing bulk proton conductivity values in BaZr0.9Y0.1O2.95, intended to be submitted to Nature Materials.

[22] Kim Sangtae and Maier Joachim: Patial electronic and ionic conduction in nanocrystalline ceria: role of space charge, J. Eur. Ceram. Soc., 2004, 24, 1919-1923.

[23] Fleig Jürgen and Maier Joachim: The impedance of ceramics with highly resistive grain boundaries: validity and limits of the brick layer model, J. Eur. Ceram. Soc., 1999, 19, 693-696.

Further publications from the project

1. S. Duval, P. Holtappels, U. Vogt, E. Pomjakushina, K. Conder, U. Stimming, T. Graule, *"Electrical Conductivity of the Proton Conductor $BaZr_{0.9}Y_{0.1}O_{3-\delta}$ Obtained by High Temperature Annealing*", **Solid State Ionics, (2007), in press** doi: 10.1016/j.ssi.2007.08.006

2. S. Duval, P. Holtappels, U. Stimming, T. Graule, *"Effect of Minor Element Addition on the Electrical Properties of $BaZr_{0.9}Y_{0.1}O_{3-\delta}$"*, **Solid State Ionics** (special issue SSI-16), submitted.

3. A. Braun, S. Duval, J.P. Embs, F. Juranyi, P.Ried, P. Holtappels, U. Stimming, T. Graule, *"Proton Diffusion in the $BaZr_{0.9}Y_{0.1}O_{3-\delta}$ Proton Conductor"*, **Physica B**, submitted.

1. S. Duval, U. Vogt, P. Holtappels, U. Stimming, T. Graule, *"Characterisation of $BaZr_{0.9}Y_{0.1}O_{3-\alpha}$ Proton Conductor Prepared with Three Different Synthesis Methods: Comparison of the Sinterability and the Conductivity"*, in preparation.

2. A. Azad, C. Savaniu, S. Tao, S. Duval, P. Holtappels, R.M. Ibberson, J.T.S. Irvine, *"On the Structural Origins of the Differing Bulk Proton Conductivity Values in $BaZr_{0.9}Y_{0.1}O_{2.95}$",* in preparation.

3. S. Duval, P. Holtappels, U. Vogt, U. Stimming, T. Graule, *"H/D Isotope Effect in Proton Conducting $BaZr_{0.9}Y_{0.1}O_{3-\delta}$"*, in preparation.